Available online at www.sciencedirect.com

ScienceDirect

Energy Procedia 00 (2017) 000–000

Energy Procedia

www.elsevier.com/locate/procedia

13th International Conference on Greenhouse Gas Control Technologies, GHGT-13, 14-18 November 2016, Lausanne, Switzerland

Changes in formation water composition during water storage at surface and post re-injection

Hong Phuc Vu[a,b,]*, Jay R. Black[a,b], Ralf R. Haese[a,b]

[a]*Peter Cook Centre for CCS Research & School of Earth Sciences, The University of Melbourne, Melbourne, Parkville, Victoria 3010, Australia*

[b]*CO2CRC Ltd, Level 1, 700 Swanston Street, The University of Melbourne, Parkville, Victoria 3010, Australia*

Abstract

Sub-surface operations such as geological carbon storage include the production, storage at surface and re-injection of formation water. Here we present results from a field-based experiment, detailing the important role of storage conditions controlling mineral dissolution and precipitation associated with the re-injection of production water. During water storage at surface, the cooling and degassing of CO_2 from produced waters and oxygenation coincides with a decrease in dissolved ions, which indicate carbonates, silicates and iron oxyhydroxides precipitate. The re-injected water is undersaturated relative to carbonate minerals under reservoir conditions leading to their dissolution in the reservoir.

Peer-review under responsibility of the organizing committee of GHGT-13.

Keywords: CO_2 sequestration; water storage, geochemical impact; field test; saturation state; mineral-fluid interactions

1. Introduction

Water is often injected or co-injected with CO_2 into reservoirs as part of enhance oil recovery (EOR) projects to improve well injectivity and help enhance oil recovery [1-4]. In natural gas projects such as coal seam gas (CSG) and shale gas projects re-injection of produced water (produced during the extraction of the natural gas) has also

* Corresponding author. Tel.: +61-390-356-769; fax: +61-383-447-761.
E-mail address: hong.vu@unimelb.edu.au

Peer-review under responsibility of the organizing committee of GHGT-13.

been implemented [5-8]. For example, the majority of produced water in United States has been re-injected into reservoirs [5, 6]. Recently, water and CO_2 have been co-injected in carbon sequestration projects to enhance CO_2 solubility and minimise CO_2 leakage [9-15]. In general, water treatment is required to remove materials that may cause the clogging of aquifers and avoid the deterioration of reservoir water's quality as well as scale and corrosive issues [16, 17]. However, the impact of water storage and treatment on changes to the geochemical composition of produced waters at surface and the subsequent dissolution and precipitation of minerals within the reservoirs has not been addressed [1, 5, 8-13, 17].

The re-injection of produced water could result in mineral dissolution and precipitation as well as the corrosion of metal in surface, down hole and injection equipment. Precipitation of carbonates (scaling issues) and corrosive issues could affect the production in reservoirs, water quality and damage the equipment [6, 18-21]. Dissolution and precipitation of minerals are strongly impacted by their saturation state [22, 23]. For example, dissolution of an example carbonate can be written as:

$$MCO_{3(s)} = M^{2+}{}_{(aq)} + CO_3{}^{2-}{}_{(aq)} \quad (1)$$

where M^{2+} may be Mg^{2+}, Fe^{2+} or Ca^{2+}. For the reaction (1), the term *log(Q/K)* is defined as the saturation index (SI), which defines the saturation state of a mineral. *Q* and *K* are ion activity products, away from and at equilibrium, respectively. Thus, SI is calculated as:

$$\log\left(\frac{Q}{K}\right) = (a_{M^{2+}} * a_{CO_3^{2-}})/(a^{eq}_{M^{2+}} * a^{eq}_{CO_3^{2-}}) \quad (2)$$

where *a* are the activities of the aqueous species, the superscript *eq* given for the system at equilibrium. Therefore, when *log(Q/K)* = 0 the system is at equilibrium, or saturation. When *log(Q/K)* > 0 the system is supersaturated, thus the reaction proceeds to the left (i.e., carbonates tend to precipitate). When *log(Q/K)* < 0 the system is undersaturated and thus the reactions proceeds to the right (i.e., carbonates tend to dissolve). The mineral saturation may be dependent on pH, temperate, pressure and redox state of the system [24-27], depending upon the type of reaction. Generally, increases in temperature and deceases in pH cause increases in mineral-dissolution rates, resulting in increases in the concentration of aqueous species and eventually the system approaches saturation [26, 27]. The impact of pressure and redox state on saturation state is dependent on specific minerals and the chemical composition of the contacting fluid. For instance, saturation state of carbonates is dependent on CO_2 solubility, which is strongly controlled by pressure and temperature [28, 29]. Increases in pressure and decreases in temperature will result in increases in CO_2 solubility [29]. If there are available divalent cations (such as Ca^{2+} and Mg^{2+}) in the fluids, the carbonates will approach saturation and eventually precipitate [28]. Redox state is only important when the system consists of redox sensitive aqueous species (such as dissolved Fe^{2+} and Fe^{3+}) and minerals (such as pyrite and siderite). For instance, Stefánsson *et al.* [25] show that precipitation of Fe(III) hydroxides and their saturation state are related to the concentration of Fe^{2+} and Fe^{3+} in natural waters of North Iceland [25].

Here we present results from the Otway 2B extension project where the impact of CO_2 impurities (O_2 and SO_2) on water-rock interactions in the Paaratte Formation of the Otway Basin, Australia was studied in a series of push-pull experiments. Two field experiments (Test 1 and Test 2) were performed to evaluate the effects of the CO_2 impurities. Test 1 (of which pure CO_2 was co-injected with water) was conducted as a baseline experiment, while Test 2 (of which CO_2 with the impurities was co-injected with water) was carried out immediately after Test 1 to evaluate the mineral-fluid interactions in the presence of the impurities. Details of the experiments and the impact of the impurities can be found in Vu *et al.* [30] and Black *et al.* [31]. In this paper, the impact of water storage prior to injection is evaluated and the role of Fe depletion will be highlighted. Aqueous speciation and reaction pathway modelling were also employed to better understand the water-fluid interactions.

2. Materials and methods

2.1. Field experiments

During the Otway 2B Extension experiment over 500 tonnes of formation water was produced and stored at the surface in three holding tanks up to 36 days before two proportions of the water were co-injected with CO_2 with and without impurities [30]. Prior to the injection, oxygen was removed from the injection water using an oxygen scavenger to reduce the dissolved oxygen concentration to less than 500 ppb. The O_2 depleted waters were mixed with CO_2 (Test 1) and CO_2 with impurities (SO_2 and O_2, Test 2) and then injected to 1.4 km-deep Paaratte Formation of the Otway Basin [30]. Four different unreactive tracers were added into the injection water to monitor fluid mixing in the subsequent back-produced water [31]. In Test 2 the concentrations of the impurities (SO_2 and O_2) are 67 ppm and 6150 ppm vol/vol, respectively. Water samples were taken during three production stages using a U-tube system [32]. For more details on sampling procedure see Vu *et al*. [30]. Once collected, the water samples were analysed on site for pH, conductivity, total dissolved solids (TDS), redox potential, dissolved oxygen and total alkalinity (TA). Water samples were also filtered through 0.45 μm cellulose acetate syringe filters before being acidified to pH 2 with concentrated ultrapure HNO_3 acid for cation analysis using ICP-OES. Proportions of the filtrates were preserved at 4°C for anion analysis using IC.

2.2. Geochemical modeling

Reaction path modelling and speciation modelling were performed using Geochemist's Workbench 9 Pro software (GWB) and thermo.com.V8.R6+ database [33]. See Vu *et al.* [30] for more details. The mineral composition employed for the modelling in Test 1 is presented in Table 1. The mineral composition for simulation in Test 2 is taken from the results of the modelling in Test 1.

Table 1. Mineral composition of the reservoir for simulation in Test 1.

Mineral	Initial volume (cm^3)
Quartz	1731.8
Albite	94.2
K-feldspar	48.9
Illite	276.9
Kaolinite	160.9
Chlorite	155.5
Calcite	8.9
Siderite	3.5
Pyrite	41.6
Hematite	4.0
Dolomite	23.9

2.3. Hydrological mixing modeling based on tracer results

Injected tracers did not behave conservatively thus it is likely that the back-produced water was a mixture of two end members, namely formation water and injection water [31]. Of the four injected tracers, Br^- and Li^+ were considered as the best tracers and selected to evaluate the fluid mixing. More details can be found in Black *et al.* [31]. The estimated concentrations in the back-produced water henceforth will be mentioned as "expected" assuming conservative behaviour. In other words, the "expected" concentrations do not account for water-rock interactions.

3. Results and discussion

3.1. Formation water, production water and injection water

Selected composition of formation water, production water and injection water is presented in Table 2. Concentrations of Na^+ and Cl^- in injection water in Test 1 and 2 were higher than in the formation water. The differences in concentrations of Na^+ and Cl^- are due to the injection water in both Test 1 and 2 being enriched in those ions as the result of the tracer addition. It is noted that the production water was contaminated by KCl, a chemical used in the completion fluid during the construction of the CRC-2 well. In comparison, concentrations of Ca^{2+}, Mg^{2+}, Si and total Fe decreased in the following order: the formation water ~ production water > injection water in Test 1 > injection water in Test 2 (Table 2). The decrease in the concentrations of Ca^{2+}, Mg^{2+}, Si and total Fe is likely due to precipitation of Fe(III) oxides/hydroxides, carbonates and silicates during the storage of the production water prior to injection. Formation water was ~ 50% saturated with dissolved CO_2 (with residual CO_2 from the previous 2B project, which was executed > 3 years prior to this study [16]), thus had a pH of 4.9 (pH calculated using the SpecE8 module of the Geochemist's Workbench 9). Once exposed to ambient conditions (i.e., the water was produced and stored at the surface), the CO_2 gas was exsolved, causing pH to increase to 6.9 (measured pH). In addition, the temperature and pressure of the water also dropped from 60 °C and 140 bar to ambient temperature and pressure, respectively. The rise in pH, the reduction in temperature and pressure as well as the oxygenation in the holding tanks at the surface led to supersaturation of several undersaturated minerals such as calcite and dolomite (calculated SI increased from -0.74 and -0.07 to 0.59 and 2.55, respectively) or further supersaturation of other minerals such as hematite, goethite and chalcedony (calculated SI increased from 6.42, 2.65 and 0.41 to 24.1, 11.6 and 1.02, respectively), causing them to precipitate. This observation is supported by the decreases in total alkalinity in injection water compared to the production water.

It is noted that the concentration of K^+ and SO_4^{2-} in the injection water of Test 1 and 2 is higher than in the production and formation water. However, the variation in K^+ and SO_4^{2-} concentration is either within or close to the concentration range of the production water, except for SO_4^{2-} concentration in the injection water Test 2 (Table 2). The reason for the increase in SO_4^{2-} concentration in the injection water Test 2 is unknown, probably due to the oxidation of reduced sulphur species during the storage.

Table 2. Selected composition of the formation water, production water and injection water in Test 1 and 2.

Sample	Na^+	K^+	Ca^{2+}	Mg^{2+}	Si	Fe	Cl^-	SO_4^{2-}	TA	TDS
Fm water	563.3	56.1	121.5	102.4	40.4	22.4	181.3	5.6	1996.3	2140.0
Prod water	616.2	66.1	136.1	124.2	41.1	24.5	178.1	6.2	2249.0	2333.0
Inj water Test 1	571.9	71.7	103.3	108.1	36.6	0.0	199.7	6.2	1581.0	2350.0
Inj water Test 2	570.3	77.7	9.6	83.4	31.1	0.0	244.9	9.3	1435.0	2300.0

Note: Fm, Prod, Inj, TDS and TA are representing for fresh formation water, production water, injection water, total dissolved solid (ppm) and total alkalinity (mg $CaCO_3$/L), respectively. All concentrations are reported in mg/L. The reported values for the production water are the averages of ten water samples, taken in ten consecutive days during the production phase. The reported values for fresh formation water are the averages of three water samples taken after the water production phase and prior to Test 1. These values are used in mixing models as mentioned in section 2.2.

3.2. Water-rock reactions and changes water composition

3.2.1. Test 1

After the co-injection of water with CO_2 in Test 1 and a soaking period, water was back-produced. The results showed very little difference between measured and expected concentrations of ions as well as TA and TDS in the back-produced water (Fig. 1 and Vu *et al.* [30]). Take Ca^{2+} concentration for example, the measured Ca^{2+} concentration fluctuated around the estimated value of ca. 100 mg/L (Fig. 1a). The consistency between measured and expected concentrations of ions as well as TA and TDS indicates that there was no or very minor acid-promoted dissolution of minerals (such as calcite) within the reservoir [30]. As mentioned in section 3.1 the saturation indices of the reactive minerals such as calcite and dolomite in the injection water were lowered by the storage conditions. This means the saturation state of these minerals in the injection water was shifted towards undersaturation from the "existing equilibrium" of the formation water. It is, thus, expected that the injection of this water would cause the dissolution of these reactive minerals to re-establish the existing equilibrium between the formation water and the reservoir minerals. The lack of evidence of mineral dissolution could be explained by low dissolution rates of the reactive minerals. It is likely that the duration of the field experiment (approximately 3 weeks) was relatively short that the dissolution of the minerals was not captured. It has been shown that not only saturation state but also kinetics controls mineral dissolution and precipitation. For example, dolomite precipitation is not widely recorded in modern marine sediments although the surface seawater is supersaturated with respect to dolomite; and a low rate of precipitation was attributed the paucity of dolomite [23 and references therein].

On the other hand, the co-injection led to a significant difference between measured and expected total Fe concentration in the back-produced water. The Fe concentration rose gradually from ca. 13 mg/L at 2.5 tonnes of water was produced then levelled off at ca. 20 mg/L after approximately 25 tonnes of water was produced. The Br^- mixing model underestimated the amount of dissolved Fe observed in Test 1, with the expected Fe concentration increasing slightly from 0.7 mg/L to 5.5 mg/L (Fig. 1b). The difference between the expected and the measured values indicates that there was an additional source contributing to the increase in dissolved Fe. The rise in Fe concentration is possibly the result of dissolution of iron-bearing minerals (such as siderite and chlorite) within the reservoir. Injected water was Fe depleted (Table 2), thus mineral dissolution is likely the consequence of a rapid response to restore the existing equilibrium between iron-bearing minerals and the formation water (i.e., to reach Fe concentration of ca. 20 mg/L). This is supported by significantly lower SI calculated for siderite ($FeCO_3$) and chlorite (chamosite-7A, $Fe_2Al_2SiO_5(OH)_4$) in the injection water (-4.98 and -18.77, respectively) compared to the formation water (0.45 and -7.29, respectively). Note that these saturation indices of the minerals in the injection water and formation water were calculated under the reservoir conditions (i.e., at 60 ºC and in the presence of saturated CO_2).

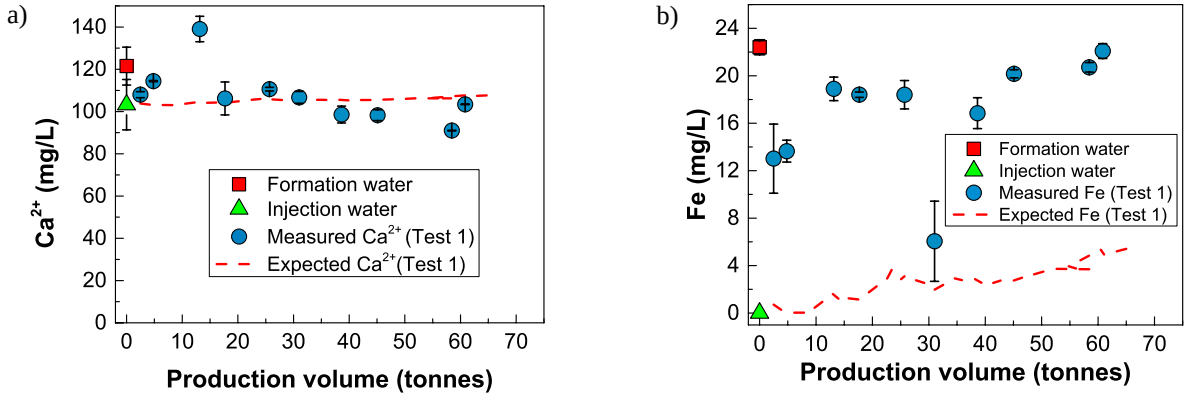

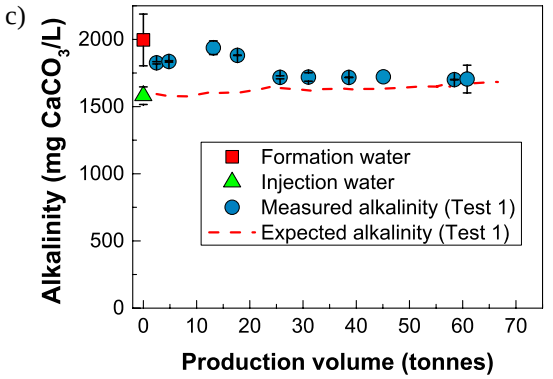

Fig. 1. Measured and expected concentration of Ca^{2+} and total Fe (a and b), and measured and expected total alkalinity in the back-produced water in Test 1 (c).

The observed mineral-fluid reactions in Test 1 and the changes in formation water chemistry are supported by the modelling results, which are presented in Fig. 2. Mg^{2+}, Ca^{2+}, Si, K^{+}, SO_4^{2-} and Fe concentrations were fairly well predicted by the model using GWB. The model predicted that a small amount of siderite (0.015 cm^3, lost volume, Fig. 2a) dissolved, leading to an increase in Fe concentration. Simultaneously, there were minor dissolution of some other minerals like calcite and dolomite and precipitation of hematite and quartz (data not shown). The magnitude of these mineral reactions was relatively small compared to siderite dissolution and reflected by the small difference between measured and predicted concentrations of ions (such as Si, Ca^{2+} and Mg^{2+}). The predicted dissolution of siderite and minor dissolution of other minerals such as calcite and dolomite are consistent with experimental data from the field experiment (see above). It was predicted that the dissolution of siderite was controlled by the existing equilibrium between formation water and Fe-bearing minerals in the reservoir. The dissolution of siderite finished after the existing equilibrium was re-established (i.e., when Fe concentration reached ca. 17.5 mg/L, Fig. 2a).

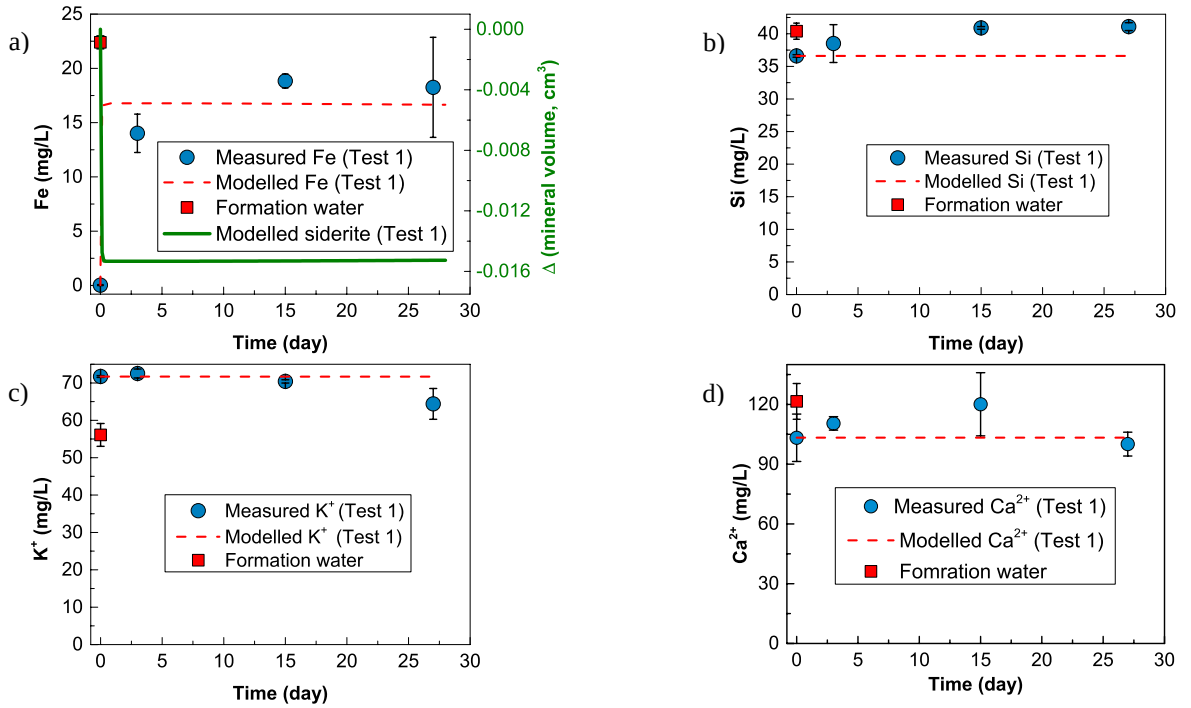

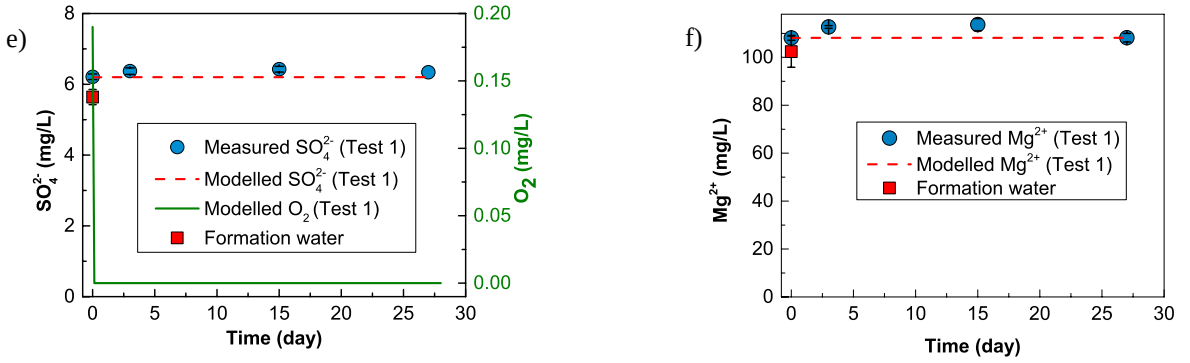

Fig. 2. Measured and predicted concentration of (a) total Fe, (b) Si, (c) K^+, (d) Ca^{2+}, (e) SO_4^{2-} and (f) Mg^{2+} in the back-produced water in Test 1.

3.2.2. Test 2

Similar to Test 1, the co-injection of CO_2 with CO_2 impurities and water in Test 2 resulted in little differences between expected and measured concentrations of ions such as Ca^{2+}, K^+, Si and Mg^{2+} as well as TA and TDS, but a large difference between expected and measured total Fe and SO_4^{2-} concentrations in the back-produced water (Fig. 3 and Vu *et al.* [30]). For instance, the expected and measured concentration of Ca^{2+} increased slightly from ca. 20 mg/L to ca. 40 mg/L, (Fig. 3a). Interestingly, the Fe concentration in Test 2 was similar to its concentration in Test 1 (Fig. 3b). In Test 2 the Li^+ mixing model underestimated the Fe and SO_4^{2-} concentrations, with the expected Fe concentration increased from 4 mg/L to ca. 10 mg/L, while the measured concentration of Fe rose moderately from ca. 9 mg/L to ca. 21 mg/L (Fig. 3b). Once again, the consistency between expected and measured concentrations of major ions (such as Ca^{2+}) suggests that the magnitude of acid-enhanced dissolution of reactive minerals was very small. The increase in measured Fe concentration compared to expected values repeatedly indicates that the additional Fe was caused by dissolution of Fe-bearing minerals (such as siderite) to re-gain the equilibrium between the Fe-bearing minerals and formation water. This is corroborated by major difference in calculated SI for siderite and chlorite (chamosite-7A) in the injection water Test 2 (-10.30 and -29.20, respectively) compared to the formation water (0.45 and -7.29, respectively). Note that the saturation indices of the minerals in the injection water and formation water were calculated under the reservoir conditions as mentioned above. The increase in SO_4^{2-} concentration was caused by oxidation of the co-injected SO_2 and oxidation of pyrite [30].

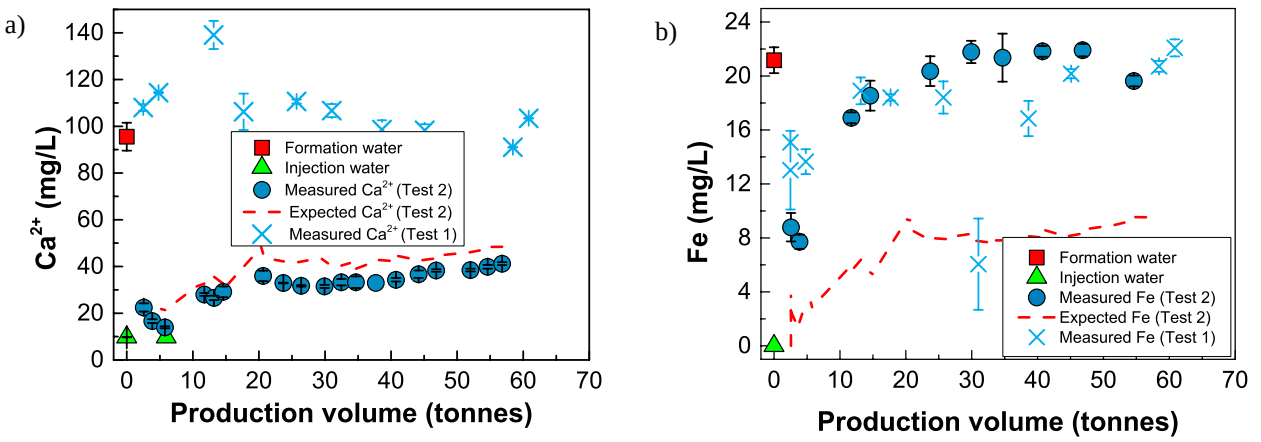

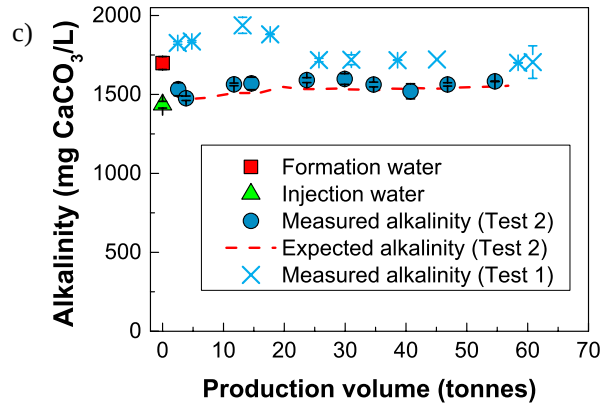

Fig. 3. Measured and expected concentration of Ca^{2+} and total Fe (a and b) and measured and expected total alkalinity in the back-produced water in Test 2 (c).

The siderite dissolution, as indicated by the experimental results, was confirmed by the reaction path modeling (Fig.4). However, the model underestimated the Ca^{2+} and Mg^{2+} concentrations in Test 2 (Fig. 4 and Vu *et al*. [30]). The disagreement between predicted and measured Ca^{2+} and Mg^{2+} concentration is caused by the mixing between the injection water and the formation water, which the reaction path model is unable to estimate [30]. The model predicted that the Fe concentration was controlled by siderite dissolution, with the predicted Fe concentration leveling off after the dissolution of siderite stopped and at that point the equilibrium between Fe-bearing minerals and formation water was re-established. Though the measured and predicted Fe concentration in Test 1 and 2 were very similar (Figs. 2-4), the predicted amount of dissolved siderite in Test 1 was one order of magnitude lower than in Test 2 (0.015 cm^3 *vs* 0.662 cm^3, respectively). It is likely that in Test 2 siderite dissolution was governed not only by the equilibrium between formation water and Fe-bearing minerals in the reservoir, but also significantly by the presence of dissolved O_2 sourced from co-injected O_2. Dissolved oxygen was predicted to oxidise aqueous Fe^{2+} to form Fe^{3+} leading to the precipitation of hematite. It is also noted that in Test 2 the oxidative dissolution of pyrite ($4.2x10^{-3}$ cm^3, lost volume) contributed partly to the equilibrium between dissolved Fe and Fe-bearing minerals in the reservoir.

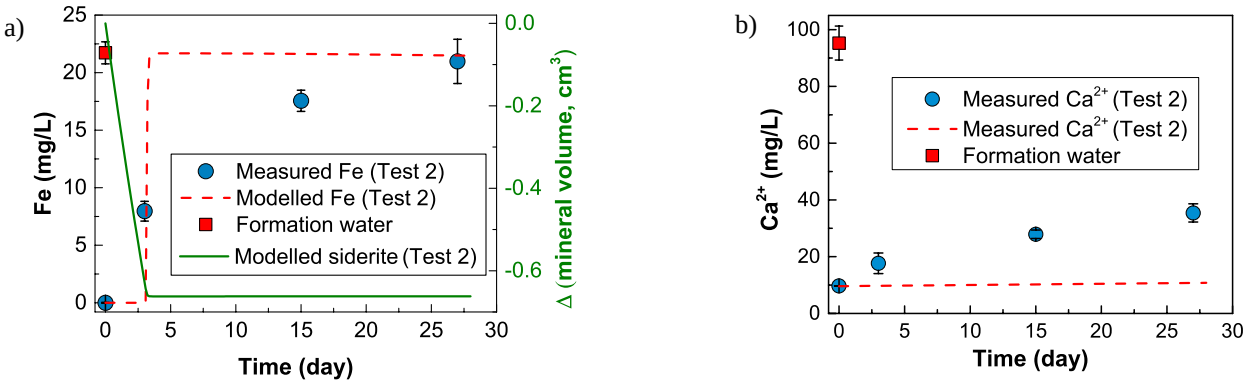

Fig. 4. Measured and predicted concentration of (a) total Fe and (b) Ca^{2+} in the back-produced water in Test 2.

4. Conclusion

CO_2 and formation water were co-injected in a field experiment executed to evaluate the impact of CO_2 impurities on water quality of a siliciclastic reservoir. Prior to the co-injection formation water was produced, stored

in holding tanks at the surface, circulated within the holding tank to ensure added tracers dissolved homogeneously and deoxygenated. Water storage and treatment under ambient conditions at the surface (i.e., increase in pH, reduction in temperature and pressure, a change in redox state from reducing to oxidising condition, residence time in the holding tanks and the circulation of production water) resulted in precipitation of carbonates, silicates and ion oxides/hydroxides. This resulted in decreases in concentration of several ions such as Ca^{2+} and Mg^{2+}, and subsequently undersaturated or further undersaturated water with respect to several reactive minerals (such as calcite) and Fe depleted injection water. Injection of this water caused the dissolution of Fe-bearing minerals (such as siderite) to re-gain the existing equilibrium between the Fe-containing minerals and the formation water. Dissolution of the other minerals such as calcite and dolomite is probably too slow to be observed during the field experiment. The dissolution of the Fe-containing minerals led to changes in water composition of the reservoir, and this impact should be taken into account when considering injection of Fe-depleted water to reservoirs. For example, in carbon capture and storage, EOR and coal seam gas projects, the injection of Fe-depleted water could induce dissolution of Fe-bearing mineral such as siderite and pyrite. Fe and trace metals (such as Mn, Cu and As) that are often associated with these Fe-bearing minerals thus would be subsequently released into the reservoirs.

Acknowledgements

We thank graduate and undergraduate students Syed Anas Ali, Cesar Castaneda Herrera, Scott Ooi for their help executing the fieldwork. The authors wish to thank the CO2CRC Ltd. for receiving regulatory approval for this experiment and for providing project oversight and management. We also thank Lawrence Berkeley National Laboratory for access to the U-tube system, the site operator (Upstream Production Solutions), Mr Rajindar Singh (CO2CRC Ltd.) and Dr Chris Spero (COSPL) for their invaluable logistical and on-site support. In addition, we thank Dr Norifumi Todaka-san (JPower) for sharing ideas and contributions to the scientific discussion. We acknowledge funding provided by the CO2CRC Ltd and Callide Oxyfuel Services Pty Ltd (COSPL). COSPL is a joint venture between Australian and Japanese companies and governments.

References

[1] C.W. Hickok, H.J. Ramsay, Jr., Case histories of carbonated waterfloods in Dewey-Bartlesville Field, in: Society of Petroleum Engineers Secondary Recovery Symposium, Society of Petroleum Engineers, 1962.

[2] H.J. Ramsay, Jr., F.R. Small, Use of carbon dioxide for water injectivity improvement, Journal of Petroleum Technology, (1964).

[3] E.J. Manrique, V.E. Muci, M.E. Gurfinkel, Enhanced oil recovery field experiences in carbonate reservoirs in the United States, in: 25th Anuual Workshop and Symposium, Collaborative Project on Enhanced Oil Recovery, International Energy Agency, Society of Petroleum Engineers, 2004.

[4] T.A. Hjelmas, S. Bakke, T. Hilde, E.A. Vik, H. Gruner, Produced Water Reinjection: Experiences From Performance Measurements on Ula in the North Sea, in: International Conference on Health, Safety and Environment, Society of Petroleum Engineers, 1996.

[5] C. Clark, V. JA, Produced water volumes and management practices in the United States, report ANL/EVS/R-09/1, in, 2009.

[6] K.B. Gregory, R.D. Vidic, D.A. Dzombak, Water management challenges associated with the production of shale gas by hydraulic fracturing, Elements, 7 (2011) 181-186.

[7] K.C. Berger, Injection of coal seam gas water into the Central Condamine Alluvium: Technical feasibility assessment, Department of Environment and Resource Management, (2011).

[8] J. Sreekanth, C. Moore, CSG water injection impacts: Modelling, uncertainty and risk analysis; Groundwater flow and transport modelling and uncertainty analysis to quantify the water quantity and quality impacts of a coal seam gas produced water injection scheme in the Surat Basin, Queensland, in, CSIRO, Australia, 2015.

[9] B. Sigfusson, S.R. Gislason, J.M. Matter, M. Stute, E. Gunnlaugsson, I. Gunnarsson, E.S. Aradottir, H. Sigurdardottir, K. Mesfin, H.A. Alfredsson, D. Wolff-Boenisch, M.T. Arnarsson, E.H. Oelkers, Solving the carbon-dioxide buoyancy challenge: The design and field testing of a dissolved CO_2 injection system, International Journal of Greenhouse Gas Control, 37 (2015) 213-219.

[10] J.M. Matter, M. Stute, J. Hall, K. Mesfin, S.Ó. Snæbjörnsdóttir, S.R. Gislason, E.H. Oelkers, B. Sigfusson, I. Gunnarsson, E.S. Aradottir, H.A. Alfredsson, E. Gunnlaugsson, W.S. Broecker, Monitoring permanent CO_2 storage by in situ mineral carbonation using a reactive tracer technique, Energy Procedia, 63 (2014) 4180-4185.

[11] S.R. Gislason, W.S. Broecker, E. Gunnlaugsson, S. Snaebjornsdottir, K.G. Mesfin, H.A. Alfredsson, E.S. Aradottir, B. Sigfusson, I. Gunnarsson, M. Stute, J.M. Matter, M.T. Arnarson, I.M. Galeczka, S. Gudbrandsson, G. Stockman, D. Wolff-Boenisch, A. Stefansson, E.

Ragnheidardottir, T. Flaathen, A.P. Gysi, J. Olssen, K. Didriksen, S. Stipp, B. Menez, E.H. Oelkers, Rapid solubility and mineral storage of CO_2 in basalt, Energy Procedia, 63 (2014) 4561-4574.
[12] R.R. Haese, T. LaForce, C. Boreham, J. Ennis-King, B.M. Freifeld, L. Paterson, U. Schacht, Determining Residual CO_2 Saturation Through a Dissolution Test-results from the CO2CRC Otway Project, Energy Procedia, 37 (2013) 5379-5386.
[13] J.M. Matter, T. Takahashi, D. Goldberg, Experimental evaluation of in situ CO_2-water-rock reactions during CO_2 injection in basaltic rocks: Implications for geological CO_2 sequestration, Geochemistry, Geophysics, Geosystems, 8 (2007) 1-19.
[14] IEAGHG, Injection strategies for CO_2 storage sites - report 2010/04, (2010).
[15] S.T. Ide, J. Kristian, O.J.F. M, Storage of CO_2 in saline aquifers: Effects of gravity, viscous, and capillary forces on amount and timing of trapping, International Journal of Greenhouse Gas Control, 1 (2007) 481-491.
[16] P.J. Davies, D.B. Gore, S.J. Khan, Managing produced water from coal seam gas projects: implications for an emerging industry in Australia, Environmental Science and Pollution Research, 22 (2015) 10981-11000.
[17] J.A. Veil, M.G. Puder, D. Elcock, J. Robert J. Redweik, A white paper describing produced water from production of crude oil, natural gas, and coal bed, methane, United States Department of Energy, Argonne National Laboratory, W-31-109-Eng-38, (2004).
[18] A. Bahadori, S. Zendehboudi, Estimation of the combined effect of temperature and carbon dioxide pressure on dissolved calcium carbonate concentration in oilfield brines, Journal of Dispersion Science and Technology, 34 (2013) 793-799.
[19] B. Dong, Y. Xu, H. Deng, F. Luo, S. Jiang, Effects of pipeline corrosion on the injection water quality of low permeability in oilfield, Desalination, 326 (2013) 141-147.
[20] B.P. McGrail, H.T. Schaef, V.A. Glezakou, L.X. Dang, A.T. Owen, Water reactivity in the liquid and supercritical CO_2 phase: Has half the story been neglected?, Energy Procedia, 1 (2009) 3415-3419.
[21] D. Brondel, R. Edwards, A. Hayman, D. Hill, S. Mehta, T. Semerad, Corrosion in the oil industry, Schlumberger, (1994).
[22] T.E. Larson, A.M. Buswell, H.F. Ludwig, W.F. Langelier, Calcium carbonate saturation index and alkalinity interpretations American Water Works Association, 34 (1942) 1667-1684.
[23] R. Arvidson, F. Mackenzie, The dolomite problem; control of precipitation kinetics by temperature and saturation state, Am J Sci, 299 (1999) 257 - 288.
[24] A. Stefánsson, S. Arnórsson, Gas pressures and redox reactions in geothermal fluids in Iceland, Chemical Geology, 190 (2002) 251-271.
[25] A. Stefánsson, S. Arnórsson, Á.E. Sveinbjörnsdóttir, Redox reactions and potentials in natural waters at disequilibrium, Chemical Geology, 221 (2005) 289-311.
[26] A. Stefánsson, S.R. Gíslason, S. Arnórsson, Dissolution of primary minerals in natural waters: II. Mineral saturation state, Chemical Geology, 172 (2001) 251-276.
[27] S.R. Gislason, S. Arnórsson, Dissolution of primary basaltic minerals in natural waters: saturation state and kinetics, Chemical Geology, 105 (1993) 117-135.
[28] J.M. Matter, P.B. Kelemen, Permanent storage of carbon dioxide in geological reservoirs by mineral carbonation, Nat. Geosci., 2 (2009) 837-841.
[29] S. Portier, C. Rochelle, Modelling CO_2 solubility in pure water and NaCl-type waters from 0 to 300 °C and from 1 to 300 bar: Application to the Utsira Formation at Sleipner, Chemical Geology, 217 (2005) 187-199.
[30] H.P. Vu, J.R. Black, R.R. Haese, The geochemical effects of O_2 and SO_2 as CO_2 impurities on fluid-rock reactions in a CO_2 storage reservoir, International Journal of Greenhouse Gas Control, (submitted).
[31] J.R. Black, R.R. Haese, H.P. Vu, Aqueous phase tracers for monitoring fluid mixing in geological reservoirs: Results from two field studies, International Journal of Greenhouse Gas Control (submitted).
[32] B.M. Freifeld, R.C. Trautz, Y.K. Kharaka, T.J. Phelps, L.R. Myer, S.D. Hovorka, D.J. Collins, The U-tube: A novel system for acquiring borehole fluid samples from a deep geologic CO_2 sequestration experiment, Journal of Geophysical Research: Solid Earth, 110 (2005).
[33] C.M. Bethke, S. Yeakel, The Geochemist's Workbench Release 9.0, Aqueous Solutions LLC, 2012.